

## F-doping effects on electrical and optical properties of ZnO nanocrystalline films

H. Y. Xu, Y. C. Liu, R. Mu, C. L. Shao, Y. M. Lu et al.

Citation: *Appl. Phys. Lett.* **86**, 123107 (2005); doi: 10.1063/1.1884256

View online: <http://dx.doi.org/10.1063/1.1884256>

View Table of Contents: <http://apl.aip.org/resource/1/APPLAB/v86/i12>

Published by the [American Institute of Physics](http://www.aip.org).

---

### Additional information on *Appl. Phys. Lett.*

Journal Homepage: <http://apl.aip.org/>

Journal Information: [http://apl.aip.org/about/about\\_the\\_journal](http://apl.aip.org/about/about_the_journal)

Top downloads: [http://apl.aip.org/features/most\\_downloaded](http://apl.aip.org/features/most_downloaded)

Information for Authors: <http://apl.aip.org/authors>

## ADVERTISEMENT



**HAVE YOU HEARD?**

Employers hiring scientists  
and engineers trust  
**physicstoday JOBS**



<http://careers.physicstoday.org/post.cfm>

## F-doping effects on electrical and optical properties of ZnO nanocrystalline films

H. Y. Xu

*Center for Advanced Opto-Electronic Functional Material Research, Northeast Normal University, Changchun 130024, People's Republic of China*  
*Key Laboratory of Excited State Processes, Changchun Institute of Optics, Fine Mechanics and Physics, Chinese Academy of Sciences, 16-Dongnanhu Avenue, Changchun, 130024, People's Republic of China*

Y. C. Liu<sup>a)</sup>

*Center for Advanced Opto-Electronic Functional Material Research, Northeast Normal University, Changchun 130024, People's Republic of China*

R. Mu<sup>b)</sup>

*Department of Physics, Fisk University, Nashville, Tennessee 372308*

C. L. Shao

*Center for Advanced Opto-Electronic Functional Material Research, Northeast Normal University, Changchun 130024, People's Republic of China*

Y. M. Lu, D. Z. Shen, and X. W. Fan

*Key Laboratory of Excited State Processes, Changchun Institute of Optics, Fine Mechanics and Physics, Chinese Academy of Sciences, 16-Dongnanhu Avenue, Changchun 130024, People's Republic of China*

(Received 2 September 2004; accepted 10 February 2005; published online 16 March 2005)

F-doped and undoped ZnO nanocrystalline films were prepared from thermal oxidation of ZnF<sub>2</sub> films deposited on a silica substrate by electron beam evaporation. The F-doped ZnO film has very low electrical resistivity of  $7.95 \times 10^{-4} \Omega \text{ cm}$  and a high optical transmittance. The study also indicated that (1) the substitutional F atoms in the film serve as donors to increase the carrier concentration and the optical band gap with respect to undoped ZnO film, and (2) F passivation reduces the known number of O<sub>s</sub><sup>2-</sup>/O<sub>s</sub><sup>-</sup> surface states and increases carrier mobility. © 2005 American Institute of Physics. [DOI: 10.1063/1.1884256]

Zinc oxide (ZnO), as a wide-band-gap semiconductor (3.37 eV) with a high exciton binding energy (60 meV), is a promising material for many optoelectronic applications, such as, ultraviolet lasers,<sup>1,2</sup> light-emitting diodes,<sup>3</sup> p-n junction devices,<sup>4</sup> thin film transistor,<sup>5</sup> solar cells,<sup>6,7</sup> acoustic devices,<sup>8</sup> and chemical and biological sensors.<sup>9</sup> For applications of transparent and conducting electrode in solar cells and thin-film transistor, the development of the low-resistive ZnO films with high transparency is important.

Studies<sup>10</sup> have showed that the surface of ZnO nanocrystals can play an important role in carrier transport. The unbonded oxygen chemisorbed on nanocrystal surface serves as traps for charge carriers, thus, increasing the interfacial potential and lowering carrier mobility. Doping with H, Mn, P, and halogens,<sup>10-13</sup> can be very effective in preventing oxygen adsorption on surfaces. For example, efforts have been made to develop an experimental strategy by incorporating F ions into ZnO nanocrystalline films via reverse doping process—oxidation of ZnF<sub>2</sub>. The results indeed show that the presence of F ions inside and outside of nanocrystals can effectively eliminate the well-known defect-associated visible emission.<sup>14</sup>

Zinc fluoride (ZnF<sub>2</sub>, 5N) was used as a source material for electron beam evaporation. ZnF<sub>2</sub> thin films were fabricated by deposition of the source materials onto silica sub-

strates. The substrate was precleaned in an ultrasonic bath with acetone. The evaporation pressure was kept at  $5 \times 10^{-5} \text{ Pa}$ , and the temperature of substrate was maintained at 400 °C during the deposition yielding an average deposition rate 70 nm/min. After deposition, the thin film was thermally oxidized at temperatures of 300, 400, and 500 °C in an ultrapure O<sub>2</sub> atmosphere. Typically, a 30 min thermal anneal was used at each set temperature. The film thickness is determined by an ellipsometer. X-ray diffraction (XRD) measurements were carried out with a D/max-RA x-ray spectrometer (Rigaku) with Cu K $\alpha$  line of 1.540 56 Å. X-ray photoelectron spectroscopy (XPS) measurements were also performed with a VG ESCALAB MK II X-ray photoemission spectrometer to identify the chemical composition of the films. Optical transmission spectra were obtained by an UV 360 spectrophotometer in the range of 190–900 nm. The resistivity  $\rho$  and Hall coefficient R<sub>H</sub> parameters were obtained by the van der Pauw method with indium metal as electrical contacts.

Figure 1 shows XRD spectra ( $\theta \sim 2\theta$ ) of an as-deposited ZnF<sub>2</sub> thin film along with the samples annealed at three different temperatures of 300, 400, and 500 °C. For the as-grown sample, the diffraction peaks reflect a typical ZnF<sub>2</sub> film with a rutile structure, suggesting the formation of a polycrystalline ZnF<sub>2</sub> film. When the sample was annealed at 300 °C, three new diffraction peaks appeared in XRD spectra at  $2\theta = 31.68^\circ$ ,  $36.24^\circ$ , and  $56.75^\circ$ , respectively. They correspond to the (100), (101), and (110) diffraction lines of ZnO

<sup>a)</sup>Electronic mail: ycliu@nenu.edu.cn

<sup>b)</sup>Electronic mail: rmu@fisk.edu

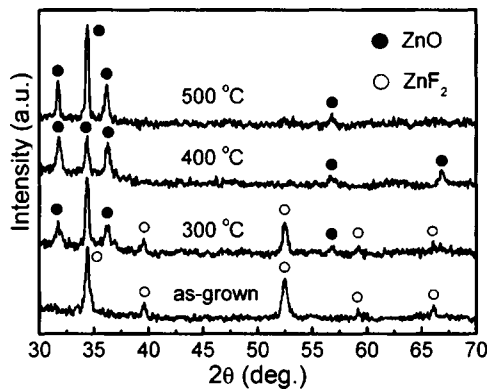


FIG. 1. XRD spectra of the as-grown ZnF<sub>2</sub> and the thin films annealed at different temperatures.

with a hexagonal wurtzite structure, respectively. XRD results clearly showed a coexistence form of both ZnF<sub>2</sub> and ZnO phases. The mix phases of the two are the result of a partial transformation from ZnF<sub>2</sub> to ZnO through thermal oxidation process. When the sample was annealed at 400 °C for 30 min, all of the diffraction peaks associated with ZnF<sub>2</sub> disappeared and a single phase of ZnO resulted. The XRD spectra also indicated that the ZnO film has no preferred orientation. As the annealing temperature was increased to 500 °C, the diffraction peaks of the ZnO film became sharper and stronger due to the improved crystal quality.

By using the well known Scherrer formula, the calculated average grain sizes of the as-grown ZnF<sub>2</sub> and ZnO films oxidized at 400 and 500 °C were 22, 21, and 30 nm, respectively.

High-resolution XPS spectra (Zn 2*p*, O 1*s*, and F 1*s*) were also recorded for all samples to identify the chemical composition of the films. The experimental details have been reported earlier.<sup>14</sup> Figure 2 shows the F 1*s* XPS bands of the films annealed at 400 and 500 °C. When the sample was annealed at 500 °C, the XPS peak of F 1*s* completely disappeared. However, XPS spectra still show a trace of F 1*s* peak when the annealing temperature was at 400 °C. The line shape of the F 1*s* spectrum is also slightly asymmetric. The Gaussian line shape fitting suggests two possible bands that are overlapped with each other. They are centered at 684.3 and 685.9 eV, respectively. It indicates that F ions may have two distinct local environments. The former is attributed to the substitutional F ions in ZnO nanocrystal, while the latter is related to the F ions associated with dangling bonds on the surface of ZnO nanocrystal.

The resistivity  $\rho$ , carrier concentration  $N$ , and Hall mobility  $\mu_H$  of abovementioned samples were measured and summarized in Table I. All films are n-types when annealed at various temperatures. However, no data were obtainable for as-prepared sample since ZnF<sub>2</sub> is an insulator. When the ZnF<sub>2</sub> film was partly oxidized at the temperature of 300 °C, the existence of the mixed phases of ZnO and ZnF<sub>2</sub> leads to measurable conduction. The highest mobility and the lowest resistivity are observed when sample annealed at 400 °C, that further supports that the film is transformed from a phase mixture of ZnO and ZnF<sub>2</sub> nanocrystalline film into a F-doped ZnO film. As expected, pure ZnO film should have higher resistivity and lower mobility values than that of F-doped film.

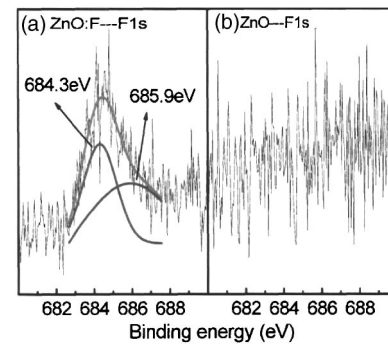


FIG. 2. P 1*s* XPS spectra of the nanocrystalline films annealed at (a) 400 °C and (b) 500 °C, respectively.

From XPS analysis of pure ZnO film (annealed at 500 °C), the elemental ratio of Zn:O was 1:0.94. The nonstoichiometry suggests the existence of oxygen vacancies and/or zinc interstitials present in the ZnO film. Photoluminescence studies<sup>14</sup> have confirmed that the oxygen vacancies are indeed the major structure defects. Therefore, for 500 °C annealed ZnO film, the donors related to the electrical conduction are oxygen vacancies and zinc interstitials known as “native donors.” On the other hand, two kinds of possible donors may be considered for 400 °C annealed sample: one is the abovementioned “native donors” and the other is substitutional F ions. Since the latter has a dominant concentration, it results in a n-type conduction with a carrier concentration of  $1.7 \times 10^{20}$  ions cm<sup>-3</sup>.

The observation Hall mobility change as a function of temperature is important. A factor of 5–10 mobility increase is observed from either the mixture phase sample (300 °C) ( $5.5 \text{ cm}^2 \text{ V}^{-1} \text{ s}^{-1}$ ) or pure ZnO (500 °C) ( $9.1 \text{ cm}^2 \text{ V}^{-1} \text{ s}^{-1}$ ) to a ZnO:F nanocrystalline film (400 °C) ( $46.2 \text{ cm}^2 \text{ V}^{-1} \text{ s}^{-1}$ ). Typically, many factors including the grain-boundary scattering, the ionized impurity scattering, the lattice vibration, and structure defects scattering can affect the carrier mobility. In the case of nanocrystalline films, the grain boundary and nanocrystal surface passivation may be considered to be the most dominant factors affecting carrier mobility. Many surface dangling bonds can chemisorb and physically trap O<sup>2-</sup> and O<sup>-</sup> ions to form O<sub>s</sub><sup>2-</sup>/O<sub>s</sub><sup>-</sup> surface system, which forms a high potential barrier on the nanocrystal surface and at the grain boundary. However, F surface passivation saturated these dangling bonds and prevented oxygen adsorption, thus, increasing mobility.

Figure 3 shows the optical transmission spectra of as-grown ZnF<sub>2</sub> together with the samples oxidized at different temperatures. Above 85% transmittance was achieved in all of the films in the visible region. In the case of the as-deposited sample, the absorption below 300 nm is largely

TABLE I. Grain size  $D$ , thickness, resistivity  $\rho$ , carrier concentration  $N$ , and mobility  $\mu_H$  of the as-grown ZnF<sub>2</sub> and the thin films annealed at different temperatures.

Samples	$\rho$ ( $\Omega \text{ cm}$ )	$\mu$ ( $\text{cm}^2 \text{ V}^{-1} \text{ s}^{-1}$ )	$N$ ( $\text{cm}^{-3}$ )	$D$ (nm)	Thickness (nm)
As-grown (ZnF <sub>2</sub> )				22	730
300 °C (ZnF <sub>2</sub> :ZnO)	$6.25 \times 10^{-1}$	5.5	$1.8 \times 10^{18}$	750	
400 °C (ZnO:F)	$7.95 \times 10^{-4}$	46.2	$1.7 \times 10^{20}$	21	800
500 °C (ZnO)	$1.56 \times 10^{-2}$	9.1	$4.4 \times 10^{19}$	30	780

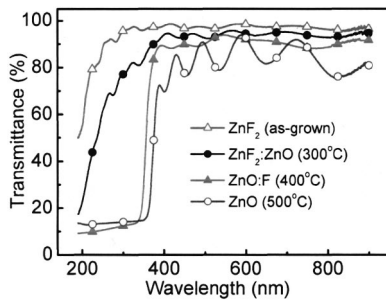


FIG. 3. Optical transmission spectra of the as-grown  $\text{ZnF}_2$  and the thin films annealed at different temperatures.

due to the silica substrate absorption. However, when the samples were annealed in oxidized environments, clear absorption onsets were observed  $\sim 360$  nm even at  $300^\circ\text{C}$  which is due to an interband transition of  $\text{ZnO}$  nanocrystals formed in the film which is confirmed as illustrated in XRD study in Fig. 1. The optical absorption edge of  $\text{ZnO:F}$  films ( $400^\circ\text{C}$ ) absorbs higher energy photons compared with that of pure  $\text{ZnO}$  film ( $500^\circ\text{C}$ ). Due to the fact that  $\text{ZnO}$  is a direct band-gap semiconductor, the optical absorption coefficient  $\alpha$  of  $\text{ZnO}$  can be estimated with the following equation:

$$\alpha = A(h\nu - E_{\text{opt}})^{1/2}, \quad (1)$$

where  $A$  is a proportional constant,  $h\nu$  is photon energy, and  $E_{\text{opt}}$  is the optical band gap. Thus,  $E_{\text{opt}}$  can be determined by plotting  $\alpha^2$  as a function of photon energy  $h\nu$ . The values of  $E_{\text{opt}}$  calculated from Eq. (2) are 3.453 and 3.285 eV for  $\text{ZnO:F}$  film and pure  $\text{ZnO}$  film, respectively. A widened optical band gap is observed for  $\text{ZnO:F}$  over pure  $\text{ZnO}$  by 168 meV.

Several factors, such as the stress effect, the quantum confinement effect,<sup>15</sup> and the Burstein–Moss effect,<sup>16</sup> can affect the optical band gap. For the nanocrystalline conducting film, the quantum confinement effect and the Burstein–Moss effect can play an important role in the shift of the optical band gap. The energy shift induced by the quantum confinement effect ( $\Delta E_{\text{QC}}$ ) can be calculated by following equation:<sup>17</sup>

$$\Delta E_{\text{QC}} = \frac{\hbar^2 \pi^2}{2d^2 \mu} - \frac{1.8e^2}{\epsilon D}, \quad (2)$$

where  $D$  is the grain size,  $1/\mu = 1/m_e + 1/m_h$  ( $m_e$  and  $m_h$  being the electron and hole effective mass, respectively) and  $\epsilon$  is the dielectric constant. For  $\text{ZnO}$ , the effective masses of electrons and holes are 0.38 and  $1.80m_0$ , respectively, and  $\epsilon = 8.75$ .<sup>17</sup> From Eq. (2), the values of  $\Delta E_{\text{QC}}$  are calculated to be 82 and 21 meV for the samples annealed at 400 and  $500^\circ\text{C}$ . The relative blueshift between the F doped  $\text{ZnO}$  and pure  $\text{ZnO}$  is estimated to be 61 meV, which may only account for 1/3 of the observed energy shift.

It is also known that for the n-type conducting semiconductor, the electronic states near the bottom of the conduction band are filled because of the high carrier concentration.

This, in turn, will induce the Burstein–Moss shift of the optical band gap ( $\Delta E_{\text{BM}}$ ).  $\Delta E_{\text{BM}}$  can be obtained by the following equation:<sup>18</sup>

$$\Delta E_{\text{BM}} = \hbar^2 N^{2/3} / (8m_e \pi^{2/3}), \quad (3)$$

where  $N$  and  $m_e$  are carrier concentration and effective mass of electrons. The values calculated from Eq. (3) were 154 and 62 meV for the samples annealed at 400 and  $500^\circ\text{C}$ . Energy shift of the two samples is 92 meV, which accounts for more than 50% of the total shift. By considering both Burstein–Moss and quantum confinement effects, the total optical band-gap shift ( $\Delta E_{\text{opt}} = \Delta E_{\text{QC}} + \Delta E_{\text{BM}}$ ) is 153 meV, which is consistent with the experimental result of 168 meV.

In summary, the  $\text{ZnF}_2$  thin film was deposited on the silica substrate by e-beam evaporation. By thermal oxidation of the  $\text{ZnF}_2$  films, the transparent conducting  $\text{ZnO:F}$  film with a wurtzite structure was formed at the annealing temperature of  $400^\circ\text{C}$ . The residue F ions present in the sample act as effective dopant and surface passivation agent, which leads to both the carrier concentration and mobility increase, and resistivity decrease. In addition, the widened optical band gap of  $\text{ZnO:F}$  film was observed in the optical transmission spectra. A simple calculation based on both Burstein–Moss and the quantum confinement effects has very successfully explained the experimental data.

This work is supported by the National Natural Science Foundation of China, Grant Nos. 60176003, 60376009, and 60278031. R.M. would also like to acknowledge the financial support from the NREL/DOE, NSF-CREST, and ARO Agencies.

<sup>1</sup>H. Cao, J. Y. Xu, E. W. Seeling, and R. P. H. Chang, *Appl. Phys. Lett.* **76**, 2997 (2000); *Phys. Rev. Lett.* **84**, 5584 (2000).

<sup>2</sup>Z. K. Tang, G. K. L. Wong, P. Yu, M. Kawasaki, A. Ohtomo, H. Koinuma, and Y. Segawa, *Appl. Phys. Lett.* **72**, 3270 (1998).

<sup>3</sup>T. Soki, Y. Hatanaka, and D. C. Look, *Appl. Phys. Lett.* **76**, 3257 (2000).

<sup>4</sup>J. M. Bian, X. M. Li, C. Y. Zhang, L. D. Chen, and Q. Yao, *Appl. Phys. Lett.* **84**, 3783 (2004).

<sup>5</sup>P. F. Carcia, R. S. McLean, M. H. Reilly, and G. Nunes, Jr, *Appl. Phys. Lett.* **82**, 1117 (2003).

<sup>6</sup>U. Rau and M. Schmidt, *Thin Solid Films* **387**, 141 (2001).

<sup>7</sup>M. H. Wu, A. Ueda, and R. Mu, *Semiconductor Quantum Dot Based Nanocomposite Solar Cells*, edited by S. Sun and Sariciftci (CRC, Boca Raton, FL, 2005), Chap. 14.

<sup>8</sup>T. Mitsuyu, S. Ono, and K. Wasa, *J. Appl. Phys.* **51**, 2646 (1980).

<sup>9</sup>Q. Wan, Q. H. Li, Y. J. Chen, T. H. Wang, X. L. He, J. P. Li, and C. L. Lin, *Appl. Phys. Lett.* **84**, 9654 (2004).

<sup>10</sup>X. M. Cheng and C. L. Chien, *J. Appl. Phys.* **93**, 1015 (2003).

<sup>11</sup>X. T. Zhang, Y. C. Liu, J. Y. Zhang, Y. M. Lu, D. Z. Shen, X. W. Fan, and X. G. Kong, *J. Cryst. Growth* **254**, 80 (2003).

<sup>12</sup>S. J. Chen, Y. C. Liu, J. Y. Zhang, Y. M. Lu, D. Z. Shen, and X. W. Fan, *J. Phys.: Condens. Matter* **15**, 1975 (2003).

<sup>13</sup>Y. Harada and S. Hashimoto, *Phys. Rev. B* **68**, 045421 (2003).

<sup>14</sup>H. Y. Xu, Y. C. Liu, J. G. Ma, Y. M. Luo, Y. M. Lu, D. Z. Shen, J. Y. Zhang, X. W. Fan, and R. Mu, *J. Phys.: Condens. Matter* **16**, 5143 (2004);

<sup>15</sup>L. E. Brus, *J. Chem. Phys.* **80**, 4403 (1984).

<sup>16</sup>E. Burstein, *Phys. Rev.* **93**, 632 (1954).

<sup>17</sup>S. Cho, J. Ma, Y. Kim, Y. Sun, G. K. L. Wong, and J. B. Ketterson, *Appl. Phys. Lett.* **75**, 2761 (1999).

<sup>18</sup>S. Fujihara, A. Suzuki, and T. Kimura, *J. Appl. Phys.* **94**, 2411 (2003).